Scientific African 15 (2022) e01066

Contents lists available at ScienceDirect

Scientific African

journal homepage: www.elsevier.com/locate/sciaf

The effect of temperature on CO_2 injectivity in sandstone reservoirs

Yen A. Sokama-Neuyam[a,*], Wilberforce N. Aggrey[a], Patrick Boakye[b], Kwame Sarkodie[a], Sampson Oduro-Kwarteng[c], Jann R. Ursin[d]

[a] Department of Petroleum Engineering, Kwame Nkrumah University of Science and Technology, PMB, Kumasi, Ghana
[b] Department of Chemical Engineering, Kwame Nkrumah University of Science and Technology, PMB, Kumasi, Ghana
[c] Department of Civil Engineering, Kwame Nkrumah University of Science and Technology, PMB, Kumasi, Ghana
[d] Department of Energy and Petroleum Engineering, University of Stavanger, 4036 Stavanger, Norway

ARTICLE INFO

Article history:
Received 5 July 2021
Revised 1 October 2021
Accepted 6 December 2021

Editor DR B Gyampoh

Keywords:
CO_2 injectivity
CCS
Thermal equilibrium
CO_2-EOR
CO_2storage

ABSTRACT

Carbon Capture, Utilization and Storage (CCUS) is a pragmatic technology that could reduce anthropogenic CO_2 and halt climate change. CO_2 injectivity is affected by several physic-ochemical interactions around the injection area of the wellbore which are temperature-dependant. There is a thermal disequilibrium between the injected CO_2 and the reservoir rock at the wellbore injection area which has not been thoroughly investigated. A pore-scale model was developed to predict the distance travelled by the injected fluid into the formation before thermal equilibrium is established. In the Snøhvit field where the well-head injection temperature is 4 °C, it was found that the injected CO_2 may attain supercritical state at bottomhole conditions, although a minimum temperature difference of about 40 °C may exist between the bottomhole fluid and the reservoir rock. Thermal equilibrium around the injection area was dependant on the wellhead injection temperature, the injection flow rate and reservoir shaliness.

Introduction

Carbon Capture, Utilization and Storage (CCUS) is a viable option to reduce CO_2 emission to the acceptable global emission reduction target and sustain exploration and production of fossil fuel [1–3]. amongst the proposed CO_2 emission reduction strategies, CCUS provides the highest emission reduction potential [4]. Injected CO_2 may be stored in depleted oil and gas reservoirs, deep saline reservoirs, unmineable coal seams or injected into active oil and gas reservoirs for Enhanced Oil Recovery (EOR) [4,5]. In terms of storage space, deep saline aquifers offer the most promising storage capacity [6–8]. A large volumetric storage potential, high well injectivity and reliable containment is needed to inject the amount of CO_2 required to reduce global emissions by appreciable margins [9]. The flow properties of injected CO_2 such as viscosity and density and its thermal properties such as heat capacity, thermal diffusivity and thermal conductivity are strongly dependant on the temperature changes along the flow stream. These properties have very strong impact on CO_2 injectivity and storage potential [10–12].

* Corresponding author at: Petroleum Engineering, Kwame Nkrumah University of Science and Technology College of Engineering, Kumasi, Ashanti, Ghana.
E-mail address: asokama@knust.edu.gh (Y.A. Sokama-Neuyam).

https://doi.org/10.1016/j.sciaf.2021.e01066

Geochemical, geomechanical and transport phenomena around the wellbore region during CO_2 injection, induce a complex interplay of different mechanisms that could impair CO_2 injectivity and reduce storage potential [9,13–15]. These phenomena depend on the physical and chemical properties of injected CO_2 which are in turn driven by reservoir temperature and pressure. The thermal changes associated with CO_2 in the well and reservoir is an area that is still being researched. It is imperative to understand the effect of CO_2 temperature changes under typical injection conditions as it is fundamental to understanding CO_2 injectivity impairment mechanisms, especially around the injection area.

Some underlying mechanisms that induce changes in CO_2 temperature in the well during injection has been previously investigated [16,17]. The injected fluid may reach the bottomhole at a temperature higher than the wellhead temperature due to heating in the well during transport. As the fluid flows from the wellhead to the bottomhole, heat is transferred from the adjacent formation through the well infrastructure to the fluid. The injected CO_2 is heated in the well due to its favourable thermal conductivity. However, depending on the initial temperature of CO_2 at the wellhead, the geothermal gradient of the formation and the depth of the well, the injected fluid may not always achieve the temperature required to attain supercritical state at the bottomhole [18,19]. To maximize injectivity and storage potential, the injected CO_2 must attain supercritical state in the bottomhole prior to flow into the reservoir. Even if the injected fluid attains supercritical state at bottomhole conditions, there may be a temperature difference between the fluid at bottomhole conditions and the reservoir. Thus, the flow and thermal properties of CO_2 may continue to fluctuate as the fluid flows from the bottomhole into the reservoir. Depending on the injection rate, the rock properties and reservoir conditions, the fluid will flow a certain distance into the reservoir before thermal equilibrium is achieved.

The thermal behaviour of injected CO_2 in the well and reservoir have also been previously investigated under various conditions. Loeve et al. [20]. have conducted a simulation to study the impact of injecting cold CO_2 into a high temperature reservoir. They found that, depending on the initial water saturation and the heat of vaporization of the resident brine, the injection area could be cooled significantly. However, the impact of the wellbore cooling on the flow properties of the injected fluid and injectivity were not studied. Gor et al. [21]. investigated the impact of additional stresses introduced by thermal disequilibrium on the caprock when CO_2 is injected at a temperature different from the reservoir temperature. They found that thermal imbalance around the caprock could induce fractures up to fracture length of 50 m within 10 years of propagation. The overall impact of these additional stresses and fracturing on the storage potential of CO_2 and containment efficiency was not thoroughly investigated. Singhe et al. [22]. developed analytical models to investigate heat transfer between injected CO_2 and the well infrastructure. They used the model to predict the temperature of injected CO_2 in the well under dynamic conditions. However, additional modelling is required to investigate the behaviour of injected CO_2 from the injection area to the reservoir. Sokama-Neuyam et al. [17]. modelled the temperature of injected CO_2 from the wellhead to the reservoir under static conditions. They found that a temperature gap exists between the injected CO_2 and the well which depends on the flow rate and injection time. Tawiah et al. [18]. presented a field observation from the Quest CCS project, where they investigated the effect of temperature on CO_2 injectivity. They observed an inverse relationship between the bottomhole temperature of CO_2 and injectivity with injectivity increasing to about 10% for bottom-hole temperature range of 21 °C – 33 °C. Hoteit et al. [23] investigated some important operational challenges encountered during CO_2 injection in low-pressure gas reservoirs. They reported fluid expansion, wellbore cooling, the Joule-Thomson effect as amongst the important wellbore phenomena that characterizes several flow assurance challenges encountered around the injection region. Jafari Raad et al. [24] investigated the non-isothermal transient behaviour of injected CO_2 at the CAMI FRS site in Alberta, Canada. They found that the presence of gas-liquid transient flow and the subsequent liquid CO_2 build-up in the wellbore could increase the bottomhole pressure significantly. Mukherjee et al. [25]. studied fluid flow and heat transfer mechanisms under non-isothermal conditions during CO_2 injection into saline reservoirs. They reported that diffusion and conduction as well as reservoir geometry and permeability anisotropy could have a significant effect on the fate of injected CO_2. However, the literature still lacks a pore-scale investigation of the thermal behaviour of injected CO_2 in the reservoir under typical injection condition to understand the microscopic mechanisms of the heat transfer process and its impact on CO_2 storage potential.

In this paper, a wellbore heat transfer model was developed to investigate the changes in CO_2 temperature from the wellhead to the bottomhole, using the Snøhvit field as a case study. A bundle-of-tubes model was then developed to investigate the pore-scale heat transfer processes during CO_2 transport into the reservoir. The objective is to track the temperature of the injected fluid until thermal equilibrium is reached between the injected CO_2 and the reservoir. The mechanisms of heat transfer under pore-scale conditions during CO_2 injection are proposed and the effect of important parameters such as CO_2 injection flow rate and the thermal properties of the reservoir rock are investigated. The study commences with the modelling process, followed by presentation of the results. The various findings are then discussed with respect to existing literature and practical implications are proposed leading to conclusions that are vital to understanding the effect of temperature on CO_2 injectivity.

Materials and methods

A brief overview of the Snøhvit field case

The Snøhvit field, located offshore the Barents Sea, produces natural gas composed of about 5–8% CO_2 [26]. At Melkøya, near Hammerfest in Northern Norway, the CO_2 is scrubbed from the gas and transported back to be reinjected into the

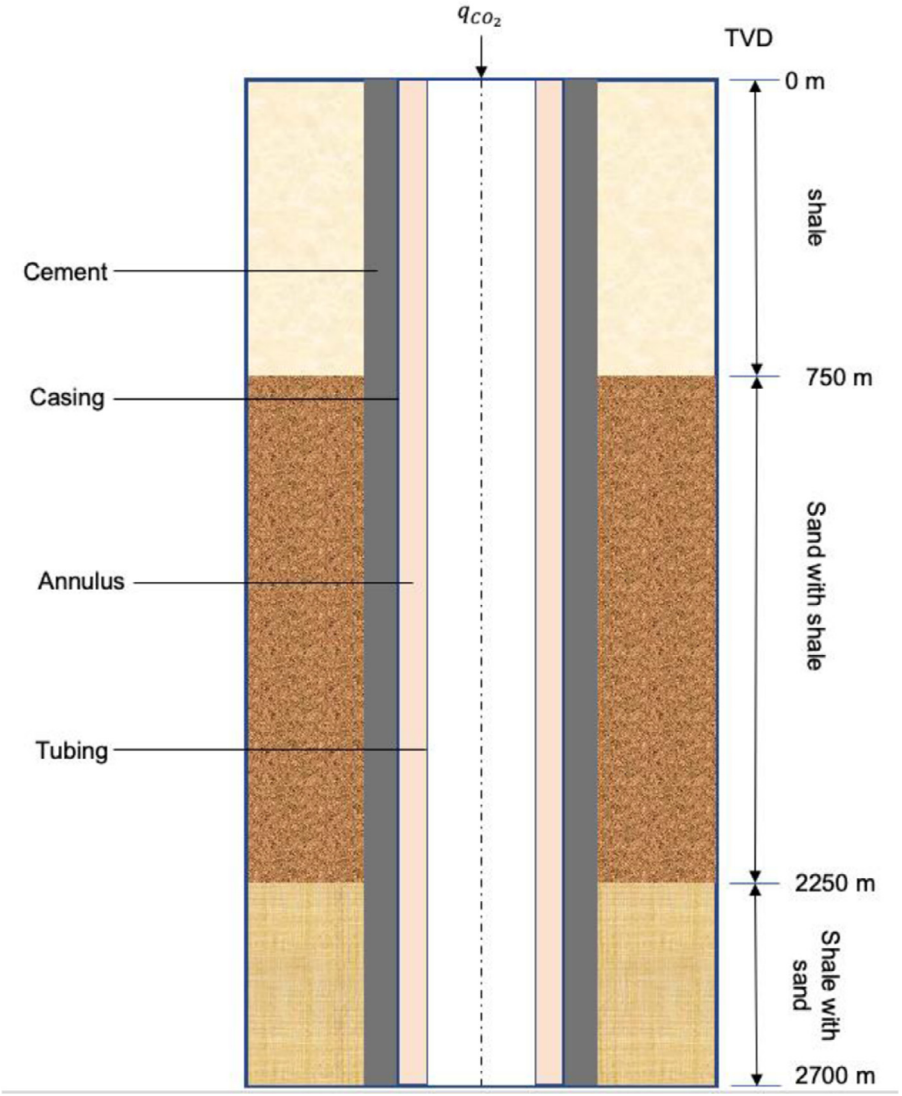

Fig. 1. Schematics of the injection well and its associated facilities.

Tubåen formation at an average injection rate of about 80 tonnes/h to be stored at a depth of about 2700 m below the seabed [27]. The CO_2 is injected at wellhead conditions of 4 °C and expected to attain supercritical phase at the reservoir conditions of 285 bar and 98 °C. The Snøhvit field consist of about four Late Triassic – Middle Jurassic formations (Fruholmen, Tubåen, Nordmela and Stø) made up of sandstone interbedded with thin shale layers. The seal and cap rock are made up of Upper Jurassic shales and thick Cretaceous shales. The porosity of the formation ranges between 10 and 15% with permeability between 1 and 659 mD. The CO_2 is injected through a single injection well with an inclination of about 27° and completed with a 4.5″ and 7″ tubing.

Wellbore heat transfer model

To model the heat transfer processes in the well, a vertical well is considered. Schematics of the injection well and the associated completion facilities are presented in *Fig. 1*. We assume that CO_2 is injected into the vertical well centred in a cylindrical reservoir at a TVD of 2700 m. From the seabed, the formation consists of 750 m of impermeable shale, about 1500 m of sand with shale and about 450 m of shale interbedded with sand as the reservoir rock [28]. It is further assumed that the well is cased-hole completed and perforated through the reservoir. Injected CO_2 flows into the well through the production casing.

Assuming steady-state flow conditions and neglecting friction effects, the temperature of injected CO_2, $T_{w_{CO2}}$ at any section of the vertical well, ΔL can be derived from the mass, momentum and energy balance equations [29]:

$$T_{w_{CO_2}} = \left(T_j + G\Delta L\right) + \left(T_{CO_{2i}} - T_j\right)e^{-\Delta L/\mathfrak{l}} + G\mathfrak{l}\left[e^{-\Delta L/\mathfrak{l}} - 1\right] \tag{1}$$

In Eq.(1), we have assumed a linear temperature variation in the formation given by:

$$T_j = T_i + G\Delta L \tag{2}$$

Where in Eq. (1) and (2), T_i is the temperature of the surrounding formation at intake, T_j is the temperature of the formation at the section of the well under consideration, $T_{CO_{2i}}$ is temperature of injected CO_2 at intake, G is the thermal gradient of the surrounding formation and $\mathfrak{l}$ is the thermal relaxation distance given by:

$$\mathfrak{l} = \frac{\dot{m}_{CO_2}C_p}{\pi U d_{ci}} \tag{3}$$

In Eq. (3), $\dot{m}_{CO_2}$ is the mass flow rate of CO_2, C_p is the heat capacity of CO_2 at constant pressure, d_{ci} is the inner diameter of the production casing and U is the overall heat transfer coefficient defined as:

$$\frac{1}{U} = \frac{1}{h_{CO_2}} + \frac{r_{ci}\ln\left(\frac{r_{co}}{r_{ci}}\right)}{k_{cas}} + \frac{r_{ci}\ln\left(\frac{r_w}{r_{co}}\right)}{k_{cem}} + \frac{r_{ci}}{k_f}f(t) \tag{4}$$

In Eq. (4), h_{CO_2} is the individual heat transfer coefficient inside the production casing, r_{ci} and r_{co} are the inner and outer radii of the production casing respectively, r_w is the radius of the well, k_{cas}, k_{cem}, and k_f are the thermal conductivity of the production casing, cement and formation, respectively and $f(t)$ is the dimensionless transient heat conduction time function of the formation given by [30]:

$$N_{Fo} \le 1.5,\ \ f(t) = 1.1281\sqrt{N_{Fo}}\left(1 - 0.3\sqrt{N_{Fo}}\right)$$

$$N_{Fo} > 1.5,\ \ f(t) = 0.4063 + 0.5\ln\left(N_{Fo}\right)\left(1 + \frac{0.6}{N_{Fo}}\right) \tag{5}$$

In Eq. (5), N_{Fo} is the Fourier number defined as:

$$N_{Fo} = \frac{\alpha t}{r_w^2} \tag{6}$$

Where, α is the thermal diffusivity coefficient of the surrounding formation, and t is time. With appropriate data, Eq. (1) can be solved to generate temperature profiles of injected CO_2 from the wellhead to the bottomhole.

The thermal behaviour of CO_2 at the bottomhole

The thermal data of the reservoir rock and fluids are very important for the temperature profile simulations. Thermal conductivity, thermal diffusivity and heat capacities are required to model heat exchange between the injected fluid and the reservoir rock. A summary of general thermal properties of the reservoir rock and fluids and the well infrastructure as well as fluid flow properties used in the study are shown in *Table 1*. Additional data for specific cases are presented in the appropriate sections.

The initial task is to estimate the bottomhole temperature of the fluid, T_{CO_2bh} given the wellhead temperature and formation intake temperature. The two main parameters studied in this section are the effect of wellhead injection temperature and the injection flow rate.

The effect of wellhead CO_2 injection temperature

To investigate the impact of CO_2 injection temperature at the wellhead, CO_2 was injected at a constant injection rate of 70 tonnes/h at three initial injection temperatures of 4 °C., 10 °C and 20 °C. The bottomhole temperature as a function of the injection time is shown in *Fig. 2*. It is observed that, generally, the temperature of injected CO_2 at bottomhole increases with wellhead injection temperature. This is intuitive because the same quantity of heat is transferred to the fluid from the wellhead to the bottomhole. The difference in temperature of the fluid at bottomhole is then approximately the difference in the wellhead injection temperatures. *Fig. 2* also shows that in the Snøhvit field where the wellhead injection temperature is 4 °C, the injected CO_2 may attain supercritical state at bottomhole conditions for all the 30 days injection time period investigated in this work. This observation agrees with available literature [27]. From *Fig. 2*, the bottomhole temperature also decreases with injection time regardless of the wellhead injection temperature. As more CO_2 is injected into the well, the same quantity of heat is transferred to a larger volume of CO_2 accumulated in the well, reducing the net heat transferred to the fluid.

Table 1
Some thermal properties of the rock and fluids, flow properties and the well infrastructure used in the simulation [27,28,36–38].

Parameter	Symbol	Value	Units
Average reservoir temperature	T_R	9 8	°C
Well vertical depth below seabed	TVD	2700	m
Formation intake temperature	T_i	4 .8	°C
Initial CO_2 injection Temperature	$T_{CO_2 i}$	4	°C
Inner radius of casing	r_{Ci}	11.43	cm
Outer radius of casing	r_{Co}	12.20	cm
Wellbore radius	r_w	16.64	cm
Average reservoir pressure	p_R	285	bar
Wellhead CO_2 injection temperature	T_{WH}	4	°C
Thermal conductivity of casing	k_{Cas}	44.3	W/m.K
Thermal conductivity of cement	k_{cem}	0.7264	W/m.K
Thermal conductivity of sandstone	k_{sand}	3.35	W/m.K
Thermal conductivity of shale	k_{shale}	1.25	W/m.K
Thermal conductivity of liquid CO_2	k_{lCO_2}	0.0927	W/m.K
Thermal conductivity of supercritical CO_2	k_{sCO_2}	0.0339	W/m.K
Specific heat capacity of liquid CO_2	C_{plCO_2}	0.819	kJ/Kg.K
Specific heat capacity of supercritical CO_2	C_{psCO_2}	0.895	kJ/Kg.K
Thermal diffusivity of sandstone	α_{sand}	1.0324×10^{-6}	m^2 /s
Thermal diffusivity of shale	α_{shale}	5.162×10^{-7}	m^2 /s
Geothermal gradient for sand	G_{sand}	0.017	K/m
Geothermal gradient for shale	G_{shale}	0.309	K/m
Average reservoir pressure	p	285	bar
Viscosity of liquid CO_2 (15 °C, 9 MPa)	μ_{lCO_2}	7.5×10^{-5}	Pa.s
Density of liquid CO_2 (15 °C, 9 MPa)	ρ_{lCO_2}	880	Kg/m^3
Viscosity of supercritical CO_2 (36 °C, 9 MPa)	μ_{sCO_2}	3.3×10^{-5}	Pa.s
Density of supercritical CO_2 (36 °C, 9 MPa)	ρ_{sCO_2}	638	Kg/m^3
Permeability of Berea Sandstone [39]	k_{sand}	80 - 120	mD
Permeability of Shale	k_{shale}	0.0001–0.0002	mD
Porosity of Berea Sandstone	ϕ_{sand}	17 - 19	%
Porosity of Shale [40]	ϕ_{shale}	4 - 7	%

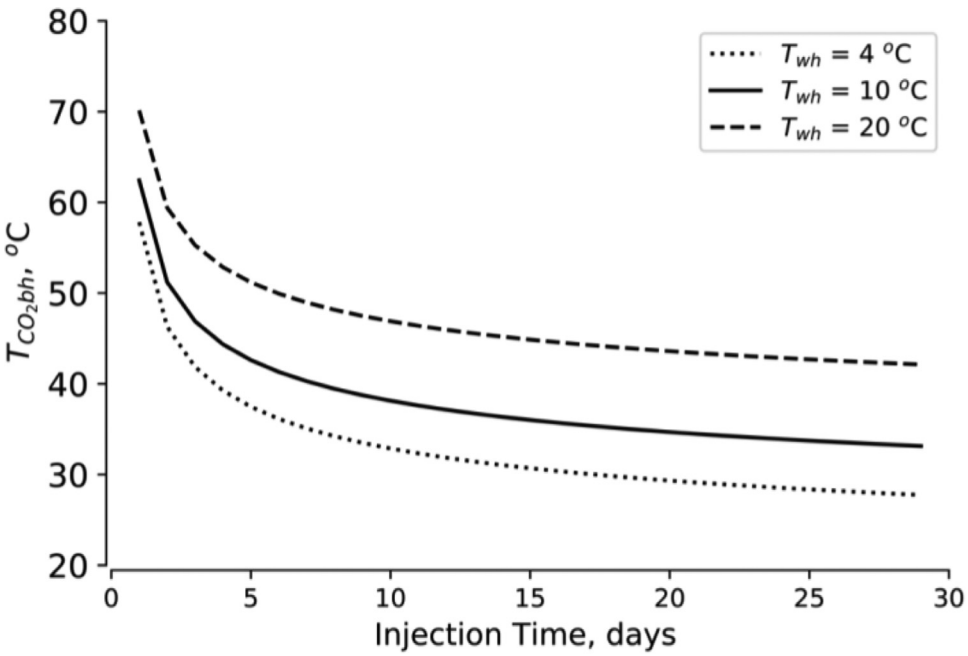

Fig. 2. The effect of initial CO_2 injection temperature on the bottomhole temperature. The temperature of the fluid at bottomhole increases with increasing wellhead injection temperature and decreases with injection time.

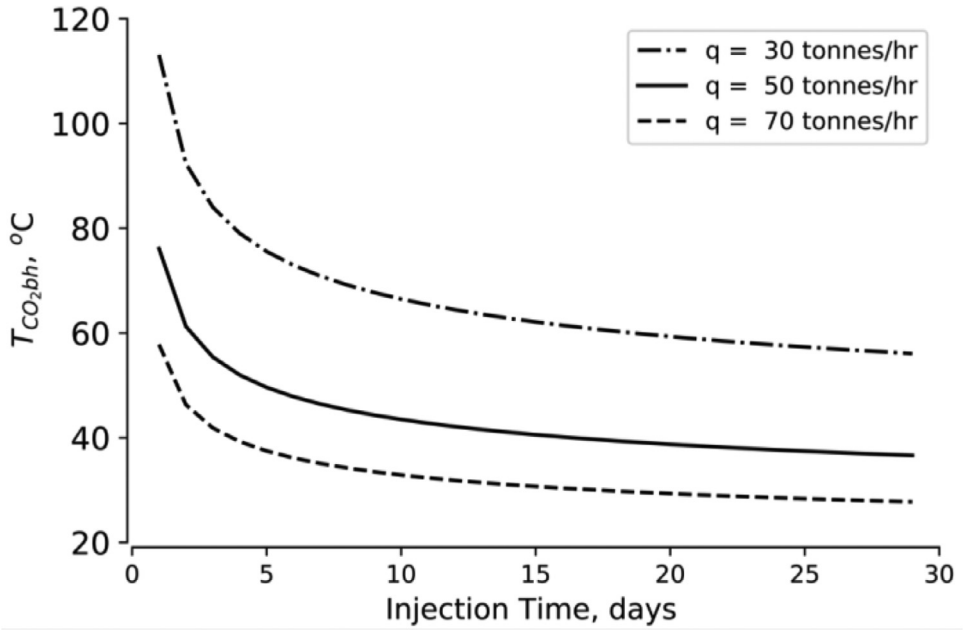

Fig. 3. The effect of CO_2 injection flow rate on the bottomhole temperature. The temperature of the injected CO_2 at bottomhole increases with decreasing injection flow rate.

The effect of CO_2 injection flow rate

To investigate the effect of CO_2 injection flow rate, the fluid was injected at constant wellhead injection temperature of 4 °C at injection rates of 30 tonnes/hr, 50 tonnes/hr and 70 tonnes/hr. Results of the simulation are presented in *Fig. 3*.

Fig. 3 shows that the bottomhole CO_2 temperature decreases as the injection rate is increased. At high injection flow rate, the retention time of injected CO_2 in the well is reduced, decreasing the quantity of heat transferred to the injected fluid in the well. Again, for all the tested flow rates, the injected CO_2 may reach the wellbore at supercritical state throughout the tested injection duration of 30 days.

In the Snøhvit field, CO_2 was injected at a wellhead injection temperature of 4 °C and at an average injection flow rate of about 70 tonnes/hr. Although at this injection condition, CO_2 reaches the bottomhole at supercritical state (temperatures above 31 °C) for all the injection duration investigated in the study, we observe that the maximum temperature the injected fluid may attain at bottomhole is about 58 °C. This bottomhole temperature is still lower than the reservoir temperature of 98 °C by a margin of 40 °C. Although the models employed in this study are simplified, we observe that the injected fluid flows into the reservoir at a temperature lower than the average reservoir temperature. The question is how far will the injected fluid travel from the wellbore into the reservoir before thermal equilibrium is achieved with the reservoir rock?

The thermal behaviour of injected CO_2 in the reservoir

The modelling work in the previous section suggests that, depending on the intake temperature and geothermal gradient, injected CO_2 may arrive in the wellbore at a temperature different from the reservoir temperature. This observation has also been confirmed in other fields during CO_2 injection [18]. Thus, a temperature gap is created between the injected fluid at bottomhole and the reservoir rock which must be gradually bridged as the fluid flows from the wellbore into the reservoir.

Considering a homogeneous reservoir rock, the heat transport in the immediate injection area of the wellbore can be adequately studied with a One-dimensional (1D) analytical model [29,31]. A pore-scale reservoir heat transfer model is developed to track the temperature of injected CO_2 as it flows from the wellbore into the reservoir.

The main assumptions of the model are as follows:

1 A fully homogenous reservoir rock
2 Steady-state heat and fluid transport in the area of investigation
3 Single phase flow of the injected fluid through a dry reservoir rock
4 The injected fluid is incompressible with constant thermal and physical properties from the wellbore to the bottomhole
5 Negligible chemical interaction between the injection fluid and the reservoir rock
6 Constant reservoir temperature in the area under consideration

Formulation of the model

For a homogeneous porous medium, the Newton's law of cooling could be adapted to model the heat transfer between the rock and the fluid but it has an obvious limitation in this case as it does not adequately incorporate the thermal properties of the reservoir rock. Therefore, we consider heat transfer in the porous medium where the linear interconnection of pores can be adequately represented by linear capillary tubes. The spaces between the capillary tubes then serves as the rock matrix. As injected fluid flows through the pores, heat is transferred between the fluid and the rock matrix. The thermal properties of the rock under consideration are built into the rock matrix and the petrophysical properties of the rock are captured in the pore size distribution.

Under steady-state conditions and constant reservoir temperature, the temperature of CO_2, T_{CO_2} in the pore of length, L can be derived from the mass, momentum and energy balance equations as [29,32]:

$$\frac{dT_{CO_2}}{dL} + \frac{1}{\lambda}T_{CO_2} = \frac{1}{\lambda}T_R \tag{7}$$

In Eq. (7), T_R is the average reservoir temperature and, λ, is the thermal relaxation distance. The overall heat transfer coefficient across the pore, U can be derived as:

$$\frac{1}{U} = \frac{r_o}{r_i}\cdot\frac{1}{h_{CO_2}} + \frac{r_o \ln\frac{r_o}{r_i}}{K_R} + \frac{r_o}{K_R}f(t) \tag{8}$$

In Eq. (8), h_{CO_2} is the heat transfer coefficient of CO_2 within the pore, K_R is the thermal conductivity of the rock, r_i is the pore radius and r_o is the radius of investigation of heat from the pore to the rock matrix defined as:

$$r_o = r_i\left(\frac{1-\phi}{\phi}\right) \tag{9}$$

In Eq. (9), ϕ is the rock porosity and $f(t)$ is the dimensionless transient heat conduction time function of the reservoir rock. With appropriate boundary conditions, Eq. (7) can be solved to obtain T_{CO_2}. In this work, it was assumed that at the wellbore sandface, $L = 0$ and $T_{CO_2} = T_{wb}$, where T_{wb} is the entry temperature of CO_2 at the sandface. The temperature of CO_2 in a single pore can then be computed.

The area of the reservoir under consideration is a cylindrical core of rock in the injection region. The pore network in the reservoir rock is modelled by a bundle of capillary tubes with varying radii, r_1, r_2, r_3,..., r_N for a total of N capillary tubes. The total number of capillary tubes in the core, N is related to the radius of the core, R, the rock porosity, ϕ and the average pore size $\bar{r}$, by [33]:

$$N = \frac{3}{4}\phi\left(\frac{R}{\bar{r}}\right)^2 \tag{10}$$

Most sandstone rocks have lognormal distribution of pores with average coordination number between 4 and 8 [34]. These properties were built into the model to give representative reservoir rock properties to the porous media under consideration.

To extend the pore-scale heat transfer model in Eq.(7) to core-scale, the rock is discretized into equal grid sections. Starting from the inlet of the core, for each section of the rock, ΔL, the temperature of injected CO_2 is calculated for each pore space. The mean temperature of CO_2 in that section of the core is then computed from a weighted average given by [17]:

$$T_{CO_2} = \frac{\sum_{n=1}^{N} r_n^2 T_{CO_2 n}}{\sum_n^N r_n^2} \tag{11}$$

In Eq. (11), $T_{CO_2 n}$is the CO_2 temperature in the pore of radius r_n. An iterative computation is performed for every pore network for the entire length of the reservoir rock to estimate the temperature of CO_2 as it flows into the rock until thermal equilibrium is established between the rock and the fluid. The equations were programmed and ran and all figures were prepared in an open-source python programming environment.

Limitations of the model

The underlying assumptions of the model discussed in Section 2.4 would have an impact on the results. The impact of some of the major assumptions are discussed. First, the model neglects reservoir heterogeneity which could further increase the retention of injected CO_2 in the reservoir and probably speed up thermal equilibrium around the injection area. However, this may have limited impact on the investigated parameters such as varying injection flow rate, reservoir shaliness and wellhead temperature. Second, incompressibility of the fluid and consequently Joule-Thomson effect was neglected which could change the transport and thermal dynamics significantly. However, the results from the model gives adequate insight about the evolution of thermal properties of the injected fluid in the reservoir which is the main objective of the work. The rate of temperature change and retention time of the injected fluid could have improved. Third, a steady-state model was assumed for the geothermal gradient which could induce continuous cooling around the wellbore. That is the main reason why the wellbore model was decoupled from the reservoir model. The wellbore model was used to estimate CO_2 temperature at the bottomhole prior to flow into the reservoir and the temperature is calculated immediately the fluid

lands in the bottomhole, which reduces the impact of the long-term cooling on the thermal behaviour of the fluid in the reservoir, making this assumption adequate for the underlying work. Fourth, constant physical and thermal properties of liquid CO_2 were assumed from the wellhead (4 °C) to the bottomhole (98 °C) which has a high tendency to underestimate the temperature of CO_2 at the bottomhole. High uncertainty of estimated CO_2 temperature at the bottomhole may exert a minimal impact on the relative distance travelled by the injected fluid in the reservoir before thermal equilibrium is attained as it will have proportional impact on the studied parameters. Another major assumption is the constant reservoir temperature around the wellbore area under investigation which under practical circumstances could vary radially away from the wellbore. This limitation imposes an uncertainty on the thermal equilibrium distance but does not reduce the usefulness of the overall results in terms of predicting thermal disequilibrium around the injection area.

Again, it is important to highlight that this is a preliminary investigation. The underlying assumptions would have a major impact on the results. However, the insight gained by the model is adequate for the purpose of the study. The model clearly provides a useful tool for understanding the thermal instabilities generated around the wellbore during CO_2 injection into a deep saline reservoir and how far these instabilities could travel away from the injection area before thermal equilibrium is established.

Results

A homogeneous cylindrical Berea sandstone rock was modelled as the main reservoir rock. The simulated area has a length of 6 m and diameter of 0.05 m. The most important properties of the reservoir rock for the current study are the petrophysical properties, thermal properties and the pore size distribution. The simulation results for each case are presented in this section. The parameters investigated include the effect of injection flow rate and the type of rock.

Effect of injection flow rate

For fluid transport in porous media, transition from Darcy to non-Darcy flow occurs at a critical modified Reynold's number, R_e between 3 and 10, where [35]:

$$R_e = \frac{\rho d_g q}{\mu A}\left(\frac{1}{1-\phi}\right) \tag{12}$$

In Eq. (12), d_g is the average grain diameter and A is the cross-sectional area of flow. Injection flow rates within the Darcy region were investigated. The CO_2 is injected into a sandstone reservoir rock at an entry temperature of 58 °C corresponding to the bottomhole temperature when CO_2 is injected at wellhead temperature of 4 °C in the simplified Snøhvit field case presented in the first part of the modelling work. Injection flow rates corresponding to modified Reynolds number of 0.2, 0.4 and 0.6 were simulated. The temperature of CO_2 in the core as a function of flow distance L_f is shown in *Fig. 4*.

The value of L_f at which the curve flattens indicates the distance travelled by the fluid into the rock before thermal equilibrium is achieved. The curve flattens when the temperature of CO_2 in the rock is equal to the reservoir temperature. *Fig. 4* shows that the flow distance traversed by injected CO_2 before thermal equilibrium is attained between the fluid and the rock increases with increasing injection flow rate. At low CO_2 injection flow rates, the injected fluid is retained in the pore spaces much longer, enabling it to exchange heat with the rock matrix more effectively. As the injection flow rate is increased from $Re = 0.2$ to $Re = 0.6$, heat transfer between the rock matrix and the rock decreases as the fluid flows faster through the rock. This explains why the fluid achieve thermal equilibrium faster at lower injection flow rate.

Effect of rock shaliness

Apart from the differences in petrophysical and petrochemical properties, the thermal diffusivity of shale is about only half of that of sandstone. This implies that, all things being equal, heat exchange between shale and the injected fluid is half of that of sandstone. Therefore, reservoir shaliness could impact the depth at which the fluid will attain thermal equilibrium with the reservoir rock. To investigate the effect of reservoir shaliness, the shale and sandstone cores were flooded with CO_2 at the same injection conditions ($Re = 0.2$ and entry temperature of 58 °C). Results of the simulation are presented in *Fig. 5*.

Fig. 5 shows that the injected CO_2 attained thermal equilibrium faster in the sandstone rock compared to the shale rock which is in agreement with theory. The thermal diffusivity of sandstone is about two times higher than that of shale. Thus, at the same injection conditions, heat will be transferred at a faster rate to the CO_2 injected into the sandstone rock compared to the shale. The petrophysical rock properties could exert some effect but the data was scaled with the Reynold's number so that the effect of pore size distribution will be negligible.

The implication on well injectivity

The steady-state well injectivity index, I for a homogeneous and isotropic reservoir can be expressed as [4]:

$$I = \frac{q}{\Delta p} = \frac{\rho_{CO_2,res}}{\rho_{CO_2,SC}} \frac{2\pi kh}{\left[\ln\left(\frac{r_e}{r_w}\right) + S\right]\mu_{CO_2,res}} \tag{13}$$

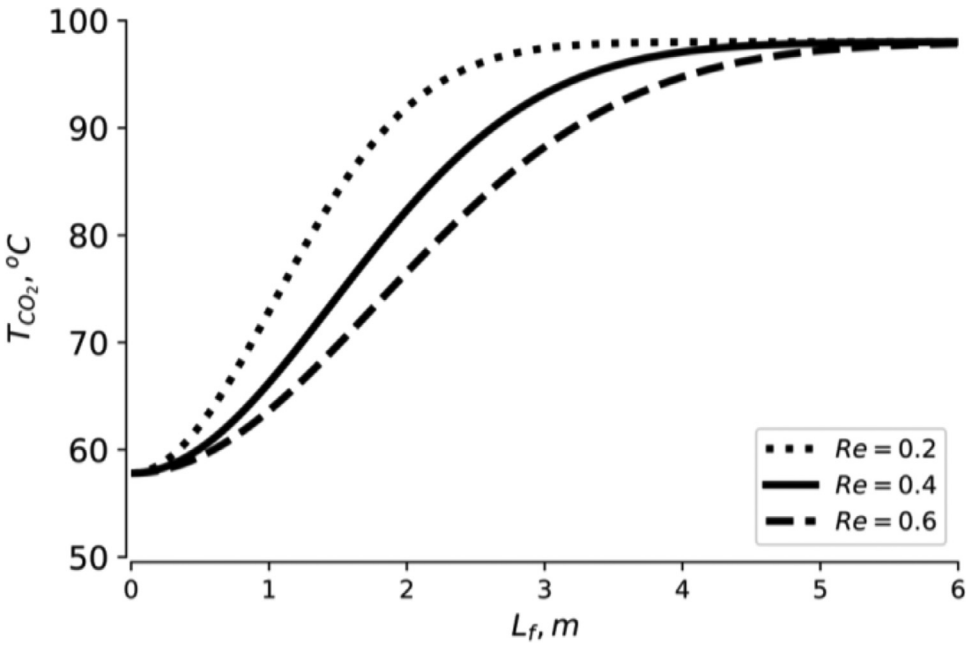

Fig. 4. The effect of injection flow rate on the depth at which thermal equilibrium is attained by the injected fluid. The injected fluid attains thermal equilibrium with the reservoir rock faster at low injection flow rate.

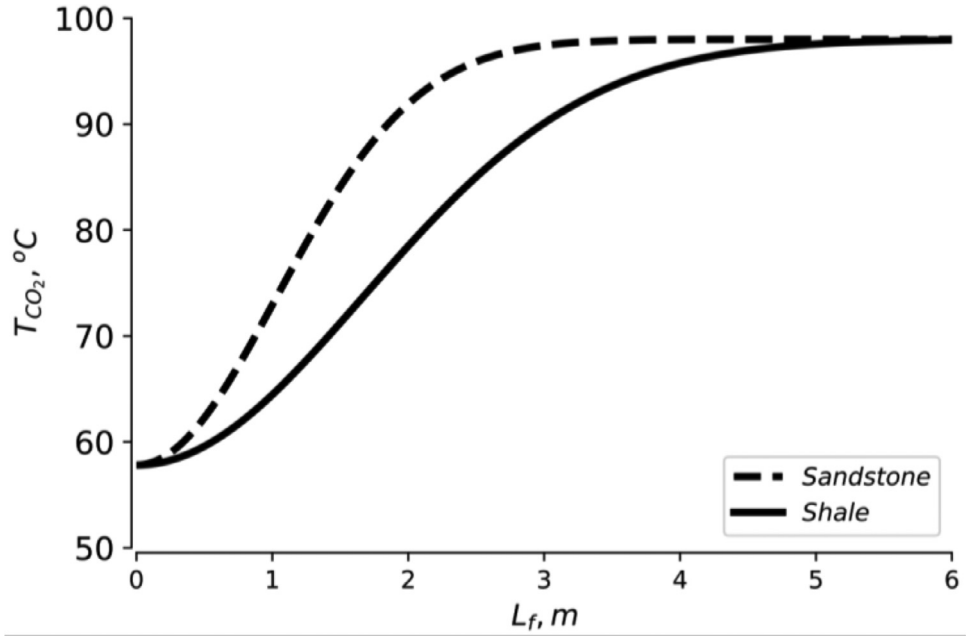

Fig. 5. The effect of rock thermal properties on the depth at which thermal equilibrium is attained by the injected fluid. The injected fluid attains thermal equilibrium faster in the sandstone rock.

In Eq.(13), q is the volumetric injection flow rate, Δp is the pressure drop, $\rho_{CO_2,res}$ is the density of CO_2 under reservoir conditions, $\rho_{CO_2,SC}$ is the density of CO_2 at standard conditions, kh is the permeability-thickness product, r_e is the radial extent of the reservoir, r_w is the well radius, S is the skin factor and $\mu_{CO_2,res}$ is the viscosity of CO_2 under reservoir conditions.

All parameters in Eq.(13) can be considered constant and independent of reservoir pressure and temperature except the density and viscosity of CO_2 in the reservoir. Thus, the equation can be further expressed as [18]:

$$I = \frac{\beta}{\left(\frac{\mu}{\rho}\right)_{res}} \tag{14}$$

Where in Eq.(14), β is then a constant given by:

$$\beta = \frac{2\pi kh}{\left[\ln\left(\frac{r_e}{r_w}\right) + S\right]\rho_{CO_2,sc}} \tag{15}$$

In Eq. (14), $(\frac{\mu}{\rho})_{res}$is the kinematic viscosity of CO_2 at reservoir conditions. Thus, the kinematic viscosity is inversely related to well injectivity index. Fluctuations of temperature in the reservoir could affect the kinematic viscosity of the injected fluid and to some extent the injectivity, especially if the temperature difference is relatively large.

Discussion

Temperature has a strong impact on the phase behaviour of CO_2 and consequently on its flow properties and well injectivity. Well injectivity is critical for the success of CO_2 injection in CCUS and Enhanced Oil Recovery (EOR) operations. CO_2 is often injected at wellhead temperature and calibrated to reach the bottomhole in supercritical state. Although the injected fluid may attain supercritical state at bottomhole conditions, there may be a temperature difference between the bottomhole fluid and the reservoir. Depending on the magnitude of this temperature difference, it may take some time for the injected fluid to attain thermal equilibrium with the reservoir rock as the fluid flows into the rock. The question is, how far will the injected CO_2 travel into the reservoir rock before thermal equilibrium is attained. Thermal fluctuations definitely have some impact on CO_2 injectivity. Insight of the thermal behaviour of CO_2 and the governing parameters could increase understanding of CO_2 injectivity impairment mechanisms especially in the wellbore injection area. A pore-scale study of the changes in CO_2 temperature in the reservoir rock was conducted, using a simplified model of the Snøhvit field as a case study. The main findings are discussed in this section with focus on their practical implications to CO_2 injection operations.

Results from the study indicates that the bottomhole temperature increases as the wellhead injection temperature is increased as the same quantity of heat is transferred to the injected fluid in the well (*Fig. 2*). However, regardless of wellhead injection temperature, the bottomhole temperature also decreases with injection time as the same quantity of heat is transferred to increasingly higher volumes of injected CO_2. In the Snøhvit field where the wellhead injection temperature is 4 °C, it was found that the injected CO_2 may attain supercritical state at bottomhole conditions for all the 30 days injection time, although a minimum temperature difference of about 40 °C may exist between the bottomhole fluid and the reservoir rock. It may not always be plausible to heat up the fluid at wellhead prior to injection. However, if the impact of the temperature difference on well injectivity justifies it, heating the fluid slightly at the wellhead prior to injection could reduce the temperature disparity around the injection area of the wellbore. However, the temperature at which the injected fluid arrive at the bottomhole was also found to decrease with increasing injection flow rate as the retention time of CO_2 in the well is reduced. This suggests that injection flow rate could also be optimised as a means of reducing the thermal disparity in the injection area.

Results from the pore-scale model suggests that the distance traversed by injected CO_2 before thermal equilibrium is attained between the fluid and the rock increases with increasing injection flow rate as the retention time of the flowing fluid in the rock is reduced, affecting heat exchange between the rock and the fluid (*Fig. 5*). As the injection flow rate is increased from $Re = 0.2$ to $Re = 0.6$, heat transfer between the rock matrix and the rock decreases as the fluid flows faster through the rock. Thermal equilibrium was attained at about 3 m for $Re = 0.2$ and about 5 m for $Re = 0.6$. The results also suggests that the injected fluid may attain thermal equilibrium faster in a sandstone rock compared to the shale rock as the thermal diffusivity of sandstone is about two times that of shale and consequently heat is transferred at a faster rate to the injected CO_2 in the sandstone rock compared to the shale. At a constant rate corresponding to $Re = 0.2$, thermal equilibrium was achieved at flow distance of about 6 m for the shale reservoir compared to about 3 m for the sandstone reservoir. This suggests that the flow rate and reservoir shaliness could impose a strong impact on temperature of the injected fluid under reservoir flow conditions.

Theoretically, the kinematic viscosity of CO_2 under reservoir conditions, $(\frac{\mu}{\rho})_{res}$is inversely related to well injectivity index. Thermal disequilibrium in the reservoir has strong impact on both CO_2 viscosity and density which could affect the kinematic viscosity of the injected fluid and to some extent the injectivity, especially if the thermal fluctuations are relatively large. A homogenous reservoir has been considered in the studies and the case study used in validation of the models was simplified. However, the insight gained provides useful understanding of the behaviour of CO_2 with temperature under typical injection conditions and its consequences on CO_2 injectivity.

Conclusion

To meet the global emission reduction target, pragmatic steps must be taken to reduce the concentration of CO_2 in the atmosphere drastically. CCUS is a promising technology capable of storing large quantities of CO_2 in geologic reservoirs including deep saline aquifers, depleted oil and gas reservoirs, unmineable coal seams and through CO_2-EOR applications. Sufficient CO_2 injectivity is required to inject large volumes of CO_2 to meet the global emission reduction target. CO_2 injectivity is affected by several physicochemical interactions around the wellbore injection area which are highly dependant on temperature. Although CO_2 injection in most projects is optimized for the injected fluid to reach the bottomhole at supercritical state, a temperature disparity may exist between the fluid at bottomhole conditions and the reservoir rock.

Depending on the magnitude of this temperature difference, it may take some time for the injected fluid to attain thermal equilibrium with the reservoir rock. The question is, how far will the injected CO_2 travel into the reservoir rock before thermal equilibrium is attained. A pore-scale model was developed to track the temperature of CO_2 in the reservoir and predict the distance travelled by the injected fluid into the formation before thermal equilibrium is established using a simplified model of the Snøhvit field as a case study. The following are the main findings of the work:

- In the Snøhvit field where the wellhead injection temperature is 4 °C, it was found that the injected CO_2 may attain supercritical state at bottomhole conditions, although a minimum temperature difference of about 40 °C may exist between the bottomhole fluid and the reservoir rock.
- The bottomhole temperature increases with wellhead uptake injection temperature and decreases with increasing injection flow rate.
- Injection flow rate was found to have a strong impact on the distance travelled before thermal equilibrium is established in the reservoir rock. Thermal equilibrium was attained at about 3 m for injection rate of $Re = 0.2$ and about 5 m for $Re = 0.6$.
- Reservoir shaliness was also found to impact thermal equilibrium. At a constant injection rate corresponding to $Re = 0.2$, thermal equilibrium was achieved at flow distance of about 6 m for the shale reservoir compared to about 3 m for the sandstone reservoir

Reservoir temperature has strong impact on the density and viscosity of injected CO_2 which have consequences on CO_2 injectivity as the injectivity index is related inversely to kinematic viscosity. These findings are based on simplified case of the Snøhvit field. However, the insight gained provides valuable understanding of the impact of temperature on CO_2 injectivity.

Declaration of Competing Interest

The authors declare no conflict of interest.

Acknowledgement

The authors would like to thank Prof. Kwasi Obiri-Danso, immediate past Vice Chancellor of the Kwame Nkrumah University of Science and Technology (KNUST), Kumasi, for his support. We also acknowledge the support of the Provost of the College of Engineering, KNUST, Prof. Mark Adom-Asamoah.

Funding

This work was not funded by any external source.

References

[1] J. Davison, P. Freund, A. Smith, Putting carbon back in the ground, IEA Greenhouse Gas R & D Programme; (2001).
[2] IEA, CO_2 capture and storage in geological formations, OECD/IEA, 2003.
[3] IEA. Technology Roadmap - Carbon capture and Storage. Technol Roadmap.
[4] R. Miri, Effects of CO_2 -Brine-Rock Interactions on CO_2 Injectivity – Implications For CCS, Uniersity of Oslo, 2015.
[5] R. Miri, H. Hellevang, Salt precipitation during CO_2 storage—A review, Int. J. Greenh. Gas Control. 51 (2016) 136–147, doi:10.1016/j.ijggc.2016.05.015.
[6] S. Bachu, D. Bonijoly, J. Bradshaw, et al., CO_2 storage capacity estimation: methodology and gaps, Int. J. Greenh. Gas Control. 1 (2007) 430–443.
[7] R.T. Okwen, M.T. Stewart, J.A. Cunningham, Analytical solution for estimating storage efficiency of geologic sequestration of CO_2, Int. J. Greenh. Gas Control. 4 (2010) 102–107.
[8] N. Singh, Deep saline aquifiers for sequestration of carbon dioxide, Int. Geol. Congr. Oslo (2008).
[9] J.M. Lombard, M. Azaroual, J. Pironon, et al., CO_2 injectivity in geological storages: an overview of program and results of the GeoCarbone-Injectivity project, Oil Gas Sci. Technol. 65 (2010) 533–539.
[10] R. Miri, H. Hellevang, Salt precipitation during CO_2 storage-A review, Int. J. Greenh. Gas Control. 51 (2016) 136–147, doi:10.1016/j.ijggc.2016.05.015.
[11] E. Azizi, Y. Cinar, Approximate analytical solutions for CO_2 injectivity into saline formations, SPE Reserv. Eval. Eng. (2013) 123–133.
[12] Y. Cinar, A. Riaz, Carbon dioxide sequestration in saline formations: part 2-Review of multiphase flow modeling, J. Pet. Sci. Eng. (2014).
[13] G. Baumann, J. Henninges, M. De Lucia, Monitoring of saturation changes and salt precipitation during CO_2 injection using pulsed neutron-gamma logging at the Ketzin pilot site, Int. J. Greenh. Gas Control. 28 (2014) 134–146.
[14] S. Grude, M. Landrø, J. Dvorkin, Pressure effects caused by CO_2 injection in the Tubåen Fm., the Snøhvit field, Int. J. Greenh. Gas Control. 27 (2014) 178–187.
[15] R. Jasinski, W. Sablerolle, M Amory, ETAP: scale prediction and contol for the Heron cluster, SPE Annu Tech Conf Exhib. Society of Petroleum Engineers, 1997.
[16] B. Ruan, R. Xu, L. Wei, et al., Thermal Modelling in and around a CO_2 Injector, Energy Procedia 37 (2013) 3283–3290, doi:10.1016/j.egypro.2013.06.216.
[17] Sokama-neuyam Y.A., Adu-boahene F., Boakye P., et al. Theoretical modeling of the effect of temperature on CO2 injectivity in. 11:1–11.
[18] P. Tawiah, J. Duer, S.L. Bryant, et al., CO_2 injectivity behaviour under non-isothermal conditions – Field observations and assessments from the Quest CCS operation, Int. J. Greenh. Gas Control. [Internet] 92 (2020) 102843, doi:10.1016/j.ijggc.2019.102843.
[19] T. Dong, L.F. Ayala, Two-phase flow models for thermal behavior interpretation in horizontal wellbores, J. Pet Explor. Prod. Technol. (2016) 45–61.
[20] D. Loeve, C. Hofstee, J.G. Maas, Thermal effects in a depleted gas field by cold CO_2 injection in the presence of methane 63 (2014) 5378–5393.
[21] G.Y. Gor, J.H. Prévost, Effect of CO_2 injection temperature on caprock stability, Energy Procedia 37 (2013) 3727–3732.
[22] T. Singhe, J.R. Ursin, J. Henninges, et al., Modeling of temperature effects in CO_2 injection wells, Energy Procedia 37 (2013) 3927–3935.
[23] H. Hoteit, M. Fahs, M.R. Soltanian, Assessment of CO_2 injectivity during sequestration in depleted gas reservoirs, Geosci 9 (2019) 1–19.
[24] S.M. Jafari Raad, D. Lawton, G. Maidment, et al., Transient non-isothermal coupled wellbore-reservoir modeling of CO_2 injection — Application to CO_2 injection tests at the CaMI FRS site, Alberta, Canada, Int. J. Greenh. Gas Control. 111 (2021) 103462.

[25] A. Mukherjee, P. Dutta, Fluid-heat dynamics and techno-economic analysis in a deep saline aquifer, Carbon Manag. 11 (2020) 593–609, doi:10.1080/17583004.2020.1840870.
[26] O. Hansen, D. Gilding, B. Nazarian, et al., Snøhvit : the history of injecting and storing 1 Mt CO_2 in the fluvial Tubåen Fm, Energy Procedia 37 (2013) 3565–3573, doi:10.1016/j.egypro.2013.06.249.
[27] A. Estublier, A.S. Lackner, Long-term simulation of the Snøhvit CO_2 storage, Energy Procedia 1 (2009) 3221–3228.
[28] A. Linjordet, R.G. Olsen, The jurassic snohvit gas field, Hammerfest Basin, Offshore Northern Norway, 1992 Chapter 22.
[29] I.N. Alves, F.J.S. Alhanati, O. Shoham, A unified model for predicting flowing temperature distribution in wellbores and pipelines, SPE Prod. Eng. 7 (1992) 363–367, doi:10.2118/20632-PA.
[30] A.R. Hasan, C.S. Kabir, Aspects of wellbore heat transfer during two-phase flow, SPE Prod. Facil. 9 (1994) 211–216, doi:10.2118/22948-PA.
[31] A.R. Hasan, C.S. Kabir, D. Lin, Analytic wellbore temperature model for transient gas-well testing, SPE Reserv. Eval. Eng. 8 (2005) 240–247, doi:10.2118/84288-PA.
[32] I.N. Alves, F.S. Alhanatl, O. Shoham, et al., Flowing Temperature Distribution (1992) 363–367.
[33] Y.A. Sokama-Neuyam, J.R. Ursin, The coupled effect of salt precipitation and fines mobilization on CO2 injectivity in sandstone, Greenh. Gases Sci. Technol. (2018).
[34] K.C. Khilar, H.S. Fogler, Migrations of fines in porous media, Springer, Netherlands, 2010.
[35] S. Ergun, Fluid Flow through Packed Columns, J. Chem. Eng. Prog. 48 (1952) 89–94.
[36] O. Hansen, D. Gilding, B. Nazarian, et al., Snøhvit: the history of injecting and storing 1 Mt CO_2 in the fluvial Tubæn Fm, Energy Procedia (2013).
[37] C. Pascal, Heat flow of Norway and its continental shelf, Mar. Pet. Geol. 66 (2015) 956–969.
[38] L. Chiaramonte, J.A. White, W. Trainor-Guitton, Probabilistic geomechanical analysis of compartmentalization at the Snøhvit CO_2 sequestration project, J. Geophys. Res. Solid Earth 120 (2015) 1195–1209.
[39] J.Q. Shi, Z. Xue, S. Durucan, Supercritical CO_2 core flooding and imbibition in Berea sandstone - CT imaging and numerical simulation, Energy Procedia 4 (2011) 5001–5008, doi:10.1016/j.egypro.2011.02.471.
[40] M. Dernaika, I.I. Dhabi, J. Walls, et al., Petrophysical Properties of Shale From Different Source Rocks in the Middle Petrophysical Properties of Shale From Different Source Rocks in the Middle East (2017).